University of Glasgow
DEPARTMENT OF
AEROSPACE
ENGINEERING

Flight Mechanics of Gyroplanes*

Dr Stewart S Houston

Internal Report No 9317

September 1993

Flight Mechanics of Gyroplanes*

Dr Stewart S Houston

Internal Report No 9317

September 1993

Department of Aerospace Engineering
University of Glasgow
Glasgow
Scotland

G12 8QQ

* Submitted to AIAA Journal of Aircraft, 2 September 1993

Flight Mechanics of Gyroplanes

S. S. Houston†

The University of Glasgow

Abstract

The class of aircraft known as gyroplanes (or autogyros) helped to pave the way for the development of the helicopter. However, they have found no application in contemporary commercial or military aviation. It is in recreational or sport flying that the gyroplane has proved popular. Most if not all designs are however homebuilts, and as a consequence little analysis of any significance has been conducted on the flight mechanics of these aircraft. This Paper presents the application of a sophisticated generic rotorcraft mathematical model to the gyroplane problem, to analyse the trim, stability and controllability of these aircraft. It is concluded that, except for longitudinal trim, the basic flight mechanics of the gyroplane are like those of the helicopter, with lightly damped rigid-body modes, extensive coupling and non-linearity in the response to control inputs. The rotorspeed degree of freedom must also be included in modelling the aircraft.

Nomenclature

A	system matrix
A_{sp}	minor of A for approximationg short-period motion
B	control matrix
C_r	controllability matrix
D	blade element drag (N)
E	eigenvector matrix of A
I_R	rotor system inertia (Nm^2)
I_{xx}	roll inertia (Nm^2)

† Lecturer
Dept. of Aerospace Engineering
The University of Glasgow
Glasgow
Scotland
G12 8QQ

I_{xz} cross product of inertias (Nm^2)

I_{yy} pitch inertia (Nm^2)

I_{zz} yaw inertia (Nm^2)

J cost function

L blade element lift (N)

M_w pitch moment derivative with respect to vertical velocity (1/s)

M_q pitch moment derivative with respect to pitch rate (1/s)

N_{bl} blade yaw moment (Nm)

R rotor radius (m)

U_p flow velocity component normal to blade element (m/s)

U_t flow velocity component tangential to blade element (m/s)

V blade element velocity (m/s)

V_f airspeed (m/s)

Z_w normal force derivative with respect to vertical velocity (1/s)

Z_q normal force derivative with respect to pitch rate (1/s)

a blade lift-curve slope (1/rad)

b number of rotor blades

c rotor blade chord (m)

dr increment of rotor blade length (m)

e blade root attachment hinge offset from hub centre

k_Ω reciprocal of rotorspeed degree of freedom time constant (1/s)

n number of turns of main rotor

p roll rate (rad/s)

$\dot{p}_i$ ith value of body x-axis angular acceleration in time history (rad/s^2)

q pitch rate (rad/s)

$\dot{q}_i$ ith value of body y-axis angular acceleration in time history (rad/s^2)

r blade element radial position from hinge (m); yaw rate (rad/s)

$\dot{r}_i$ ith value of body z-axis angular acceleration in time history (rad/s^2)

t_1, t_2 trim and linearisation algorithm time range (s)

u translational velocity along body x-axis (m/s)

$\dot{u}_i$ ith value of body x-axis translational acceleration in time history (m/s^2)

$\underline{u}$ control vector

v translational velocity along body y-axis (m/s)

$\dot{v}_i$ ith value of body y-axis translational acceleration in time history (m/s^2)

w translational velocity along body z-axis (m/s)

$\dot{w}_i$ ith value of body z-axis translational acceleration in time history (m/s^2)

$\underline{x}$ state vector

$\dot{\underline{x}}$ state vector acceleration

$\underline{x}_{cg}$ centre of mass position vector with respect to airframe reference (m)

x_{hub} hub x axis

$\underline{x}_{hub}$ hub position vector with respect to airframe reference (m)

$\underline{x}_i$ ith value of state vector in time history

$\dot{\underline{x}}_i$ ith value of state vector acceleration in time history

$\underline{y}_{trim}$ trim state vector

$\underline{z}$ transformed state vector

$\dot{\underline{z}}$ transformed state vector acceleration

Δt time increment in numerical integration (s)

Λ diagonal matrix of eigenvalues of A

Ω rotorspeed (rad/s)

Ω_e equilibrium rotorspeed (rad/s)

Ω' perturbation rotorspeed (rad/s)

$\dot{\Omega}$ rotor angular acceleration (rad/s^2)

$\dot{\Omega}_i$ ith value of rotor angular acceleration in time history (rad/s^2)

α blade element angle of attack (rad)

δ blade element drag coefficient

δ_r rudder angle (rad)

δ_t propeller blade root pitch angle (rad)

$\delta \underline{x}_j$ state vector perturbation

$\delta \underline{u}_j$ control vector perturbation

ϕ roll angle (rad)

θ pitch angle (rad)

θ_{1c} lateral cyclic pitch angle (rad)

θ_{1s} longitudinal cyclic pitch angle (rad)

ρ air density (kg/m^3)

ψ blade azimuthal position about shaft (rad)

Introduction

There are a wide range of configurations in the family of aircraft known as rotorcraft. The helicopter is the most common type, finding widespread application in commercial and military aviation. The gyroplane however, is an increasingly popular machine in sport and recreational flying, having found no practical application in contemporary commercial or military roles. The gyroplane did however help to pave the way for the development of the helicopter, introducing cyclic pitch control and blades attached to the rotor hub by means of a hinge, Ref. 1.

Currently, most if not all types of gyroplane are in the homebuilt category. As a consequence, the depth of analysis of the type's flight mechanics is limited by the absence of the mathematical modelling and simulation facilities available to major aerospace organisations. The study of gyroplane flight mechanics is however timely, in the light of the accident rate suffered by the aircraft. For example, in the U.K., there were 6 fatal gyroplane accidents in the period 1989-91, Ref. 2.

Background

The helicopter integrates the functions of lift, propulsion and control in the main rotor, while the gyroplane separates propulsion from lift and control. The key difference between the two configurations however, is that the helicopter has a torque applied to the main rotor shaft in order for

it to rotate and hence provide lift; the gyroplane has no torque applied, relying instead on the flow of air through the rotor produced by virtue of forward speed to rotate it. Therefore, the gyroplane has no still-air hover capability, which also means that it has no still-air vertical take-off and landing capability. Moreover, its low-speed capability is limited to manoeuvres in a direction determined by the propulsive force thrust axis, which is aligned with the aircraft fore-and-aft direction. Without a 'steerable' propeller, the gyroplane cannot fly backward or sideways.

The configuration therefore lacks the characteristics of the helicopter that have made it so popular a rotating-wing configuration. In some respects, the gyroplane could be considered to be a rotary-wing aircraft without any of the unique benefits in terms of hover and low-speed manoeuvrability that rotating wings convey to the helicopter.

The current technical level of rotorcraft mathematical modelling for simulation is such that blades are individually represented as bodies, with the aerodynamic and inertial loading built up from summed elements distributed along the blade radius. The mathematical description of the model used for the results in this Paper is contained in Ref. 3. The model is generic, and its key features are summarised in Table 1. The full range of rotorcraft, from helicopter (in tandem, coaxial or single main and tail rotor forms) to tilt rotor or even the gyroplane can be simulated with appropriate data. For the gyroplane application, the second rotor in the model is configured as a propeller. The software implementation of the model allows calculation of time response to a general set of initial conditions, calculation of the response to control inputs and atmospheric disturbances, calculation of the trim required to maintain a given flight state, and a linearisation routine which calculates stability and control derivatives for a six or seven degree-of-freedom rigid-body representation of the aircraft.

Theory of Gyroplane Flight

In this section the physical principle of the production of lift by a gyroplane is described and contrasted with the helicopter.

Figure 1 shows the velocities and forces acting on a blade element when the rotor is operating in helicopter mode. It is clear that both lift and drag have components acting along the negative hub x direction, i.e. opposing the motion of the blade element. Therefore, a torque must be applied to the rotor shaft, by the engine or engines, to balance the torque arising from the lift and drag.

Table 1 Mathematical model description

Model item	Characteristics
Rotor dynamics (both rotors)	• up to 10 individually-modelled rigid blades • fully-coupled flap, lag and feather motion • blade attachment by offset hinges & springs • lag damper
Rotor loads	• aerodynamic and inertial loads represented by up to 10 elements per blade
Blade aerodynamics	• lookup tables for lift and drag as function of angle-of-attack and Mach number
Wake model	• momentum-derived dynamic wake model • uniform and harmonic components of inflow • rudimentary interaction with tail surfaces • ground effect
Transmission	• coupled rotorspeed and engine dynamics • up to 3 engines • geared or independently-controlled rotor torque
Airframe	• fuselage, tailplane and fin aerodynamics by lookup tables or polynomial functions
Atmosphere	• International Standard Atmosphere • provision for variation of sea-level temperature and pressure

The situation for the rotor acting in gyroplane mode or autorotative flight, is shown in Figure 2. Here, the lift and drag force components in the hub x direction are in balance, and no torque is required to be applied to the shaft. This situation can only arise if the inflow angle changes sign i.e. the inflow is up through the rotor, opposite to the helicopter in powered flight.

Associated with the balance of lift and drag required to produce autorotative flight, is the rotorspeed degree of freedom. Unlike the helicopter, no torque is applied to the rotor shaft by the engine, controlled either by the pilot or an automatic system to provide a nominally constant

rotorspeed. An understanding of the behaviour of the rotorspeed degree of freedom is therefore of as much interest as the nature of autorotative flight itself.

A simple model of rotorspeed behaviour can be constructed from the full equations given in Ref. 3. From Newton's 2nd. Law,

$$I_R \dot{\Omega} = N_{bl} b$$

The aerodynamic torque can be derived from Figure 2, neglecting any blade in-plane (lag) or out-of-plane (flap) displacements, as

$$N_{bl} = 1/2 \rho c e R \int_{eR}^{R} V^2 (a\alpha\phi - \delta) dr$$

where

$$\alpha = \theta + \phi$$
$$\phi \approx U_p / U_t$$
$$V^2 = U_p^2 + U_t^2$$
$$U_t = V_f \sin \psi + \Omega r$$

The rotorspeed equation can be expressed in linearised, small perturbation form by assuming that the periodic terms in the aerodynamic torque do not affect stability and act simply as a forcing function, by neglecting products of small quantities, and assuming that $\Omega = \Omega_e + \Omega'$. The result is a linear ordinary differential equation with a constant coefficient, i.e.

$$\dot{\Omega}' = k_\Omega \Omega'$$

where

$$k_\Omega = -\rho c e \Omega^2 R^4 \delta (1 - e^3) b / (6 I_R)$$

The sign of the coefficient k_Ω determines the stability of the rotorspeed to perturbations, and its magnitude determines the rise time. For the gyroplane configuration simulated in this Paper, the coefficient is approximately -0.15, indicating a stable mode with a rise time of 4-5 s.

Simulation of Rotorcraft with Individually Modelled Blades

Since the rotor blades are modelled individually, the governing equations of motion are periodic, even in an equilibrium (trimmed) flight condition. This is illustrated in Figure 3 which shows the vertical acceleration at the gyroplane's centre of mass in steady level flight at 80 knots, during three complete revolutions of the rotor. This behaviour presents special problems, particularly in seeking a trimmed flight state solution. Several authors have tackled this problem, e.g. Kim (Ref. 4). More recently, descriptions of periodic trim methods and results have been presented by McVicar (Ref. 5) and Achar & Gaonkar (Ref. 6). The approach taken with this model will now be described.

Trim algorithm

The trim method that is used with the model is simple but has proved to be effective in calculating the control positions and attitudes required to maintain a general equilibrium flight state. As will be seen it is an approximate method, but the approximation to the trim has been found to be very good indeed.

The problem for the gyroplane is stated as:
given a general steady flight condition defined by airspeed, climb rate, turn rate, heading and track, find the steady, time-invariant vector

$$\underline{y}_{trim} = [\, \theta_{1s}\ \theta_{1c}\ \delta_r\ \delta_t\ \varphi\ \theta\ \Omega\,]^T$$

such that the function

$$J = \sum_i^n \underline{\dot{x}}_i = 0$$

where

$$\underline{\dot{x}}_i = [\, \dot{u}_i \; \dot{v}_i \; \dot{w}_i \; \dot{p}_i \; \dot{q}_i \; \dot{r}_i \; \dot{\Omega}_i \,]^T$$

The subscript i denotes the ith point in a discrete time history of n points, where

$$n = (t_2 - t_1) / \Delta t$$

For rotorcraft in general, there are an integer number of complete revolutions of both rotors in the interval $(t_2 - t_1)$. This is necessary because the cost function J is proportional to the sum of the mean forces and moments acting on the airframe during the interval. For the gyroplane, this is not a restriction since the propeller produces negligibly small periodic forces and moments. The value of t_1 is chosen to be greater than the settling time of the slowest mode, typically the blade in-plane (lag) dynamics.

The cost function J is minimised using a standard least-squares method. An initial value of $\underline{y}_{trim}$ is chosen and J calculated. During the time interval $(t_2 - t_1)$ the acceleration vector $\underline{\dot{x}}_i$ is not integrated with respect to time. The aircraft is therefore constrained to fly a particular trajectory with a particular attitude and rotorspeed, defined by the current value of the vector $\underline{y}_{trim}$ in the iterative least-squares scheme. The resulting forces and moments acting on the airframe over the time interval $(t_2 - t_1)$ are calculated. If $J \neq 0$ then a new selection of $\underline{y}_{trim}$ is made, and the process repeated until $J = 0$.

The relatively lightly or negatively damped rigid-body and rotorspeed modes are therefore suppressed at each stage in the minimisation, including the ultimate stage in the trim calculation process. Therein lies the approximate nature of this method, since this is an unrealistic situation. The trim state is defined by time-invariant flight condition, aircraft attitude and rotorspeed, whereas in reality the periodic nature of the forcing applied to the airframe will result in a periodic rather than time-invariant trim. However, it has been found that having calculated the trim using the method

described, "releasing" the trimmer (i.e. integrating the vector $\underline{\dot{x}}_i$ with respect to time) results in a periodic attitude, flight condition and rotorspeed that even with lightly and negatively damped rigid-body and rotorspeed modes, takes a considerable amount of time to diverge significantly from what is then, in effect, a pseudo-trim state, Figure 4.

Linearisation algorithm

The trim method is readily extended to the calculation of stability and control derivatives. The linear 7 degree-of-freedom (6 rigid-body plus rotorspeed) in state-space form is

$$\underline{\dot{x}} = A\underline{x} + B\underline{u}$$

where $\underline{x} = [u\ v\ w\ p\ q\ r\ \phi\ \theta\ \varphi\ \Omega]^T$ and $\underline{u} = [\ \theta_{1s}\ \theta_{1c}\ \delta_r\ \delta_t]^T$. Then, given $\underline{y}_{trim}$ the cost function J is repeatedly recalculated with each state and control in the 7 degree-of-freedom model structure sequentially and individually perturbed by a small amount. Then, for a single-sided difference method

$$A_j = \sum_i^n \underline{\dot{x}}_i(\delta\underline{x}_j) / (n\delta\underline{x}_j)$$

$$B_j = \sum_i^n \underline{\dot{x}}_i(\delta\underline{u}_j) / (n\delta\underline{u}_j)$$

Results

Currently, gyroplanes tend to have a two-bladed main rotor of teetering-type articulation, and a two-bladed fixed-pitch propeller. In order to render the current study non-specific to a type or types, the main rotor was configured as a three-bladed type with offset flap, lag and feather hinges. The propeller was configured as a three-bladed constant-speed unit. The geometry and mass properties are otherwise similar to current machines. Table 2 contains the leading particulars of the configuration simulated.

Airframe aerodynamics are configuration-specific for any type of aircraft and it was for this reason that they were neglected in this study. This includes propeller slipstream effects on the rudder. Therefore, the flight mechanics of the basic vehicle configuration are examined. The results are still applicable to gyroplanes in this weight category.

Table 2 Configuration leading data

Parameter	Description
Mass	300 kg
I_{xx}	480 kg m^2
I_{yy}	1500 kg m^2
I_{zz}	900 kg m^2
I_{xz}	105 kg m^2
$\underline{x}_{cg}$	(0.25,0,0) m
Blade radius	3.6 m
Blade mass	7.2 kg
Distribution	uniform
Twist	0 deg
Chord	0.2 m
Airfoil section	NACA 0012
Mach number validity	0-0.8
Angle-of-attack range	±21 deg
Number of elements	9
Hinge offset	0.025
Direction of rotor rotation	Clockwise viewed from above
Shaft tilt (aft)	5 deg
$\underline{x}_{hub}$	(0,0,-1) m
Rudder area	2 m
Lift curve slope	3.8 /rad
Propeller rpm	2500
Blade twist	0 deg

Trimmed flight requirements

Figures 5, 6 and 7 show the control angles, aircraft attitudes and rotorspeed required to trim the gyroplane in level flight between 30 and 80 knots. This speed range was determined by the fact that a viable equilibrium flight state could not be achieved below 30 knots because of blade aerodynamic limits. Above 80 knots the power required exceeded that available from a range of small piston engines.

In Figure 5, it can be seen that the longitudinal cyclic required to trim is increasingly negative with increasing forward speed, indicating positive static stability. However, it is very weak, the control angle required changing by only 1 deg. The lateral cyclic pitch is also negative, becoming more so with increasing speed. This is attributed to the pitch required to balance the asymmetry in lift produced with a rotor system in forward flight, and is of a sign consistent with rotor direction of rotation. The rudder angle required increases with decreasing speed due to the reduction in dynamic pressure. Rudder angle is required to balance the sideforce produced by the lateral cyclic pitch . In reality, the rudder angle required at low speeds is likely not to be as significant because of propeller slipstream effects. (The model calculates a propeller induced velocity of almost 20 knots at an airspeed of 30 knots).

In Figure 6, it can be seen that the pitch attitude decreases with increasing airspeed, from a value of almost 20 deg at 30 knots. In this regard the gyroplane is similar to a fixed-wing aircraft, and the rotor can be viewed as a circular wing that will eventually stall when the airspeed is too low. The roll attitude however is non-zero, akin to the situation found with the helicopter, and this is due to the lateral tilt of the main rotor disc required to balance the lift asymmetry between advancing and retreating sides of the disc.

Figure 7 shows the rotorspeed required to produce trimmed flight. As can be seen, it increases with increasing forward speed, which is intuitively correct since increasing airspeed will increase the mass flow of air through the rotor. Although the rotorspeed is almost double that of

contemporary helicopters, at 80 knots it still results in tip speeds on the advancing side of the rotor of typical hovering helicopter values of about Mach 0.65.

Modes of motion

The eigenvalues of the matrix A determine the stability of the quasi-steady rigid-body modes. There are four longitudinal and five lateral-directional eigenvalues, together with one arising from the rotorspeed degree of freedom. Figure 8 shows these eigenvalues across the 30-80 knots speed range at intervals of 10 knots. Each mode of motion is given a different symbol. For clarity, particularly because of the low-modulus eigenvalues, teach speed point has not been identified individually, since the figure is intended mainly to show qualitatively the nature of gyroplane motion in level flight. There are two large modulus modes, one aperiodic (denoted by crosses) and one oscillatory (denoted by circles). The other modes are of low modulus and are predominantly stable, although the mode shown by solid diamonds is unstable. It should be noted however that all the other low modulus modes (denoted by squares and triangles) are unstable at 30 knots, a relatively substantial migration to the stable left-half plane taking place when the speed is increased from 30 to 40 knots.

It is necessary to examine the eigenvectors associated with each eigenvalue of the matrix A if the character of these modes (in terms of state variables) is to be established. The 80 knot case is considered for illustrative purposes although analysis of the other speeds results in the same conclusions. The two large modulus modes are examined in detail, together with the unstable low modulus one. Table 3a shows that the large modulus oscillatory mode is most like a helicopter or aeroplane dutch roll, with sideslip velocity v being the dominant translational velocity in the motion, and roll and yaw being the dominant angular velocities with yaw rate lagging roll rate by about 90 deg. Table 3b shows the other large modulus mode to be predominantly longitudinal in nature. Vertical velocity is the dominant rigid-body motion, and there is substantial rotorspeed response present also. Table 3c shows that the unstable low modulus mode is also mainly longitudinal in nature. Dominant translational velocities are u and w while q is the most significant angular velocity. This mode is therefore most like a helicopter or aeroplane phugoid in nature (the instability

suggests however it to be most like the unstable phugoid found with helicopter response), although there is substantial rotorspeed response in this mode also.

Table 3a Large modulus oscillatory mode character

Eigenvalue -0.4243+3.9088i		
State	**Modulus**	**Phase (deg)**
u	0.0210	46.4
v	0.9774	0
w	0.1765	7.2
p	0.0505	359.0
q	0.0156	46.0
r	0.0878	269.1
ϕ	0.0129	258.3
θ	0.0036	303.7
φ	0.0224	172.8
Ω	0.0440	274.7

Table 3b Large modulus aperiodic mode character

Eigenvalue -2.8248		
State	**Modulus**	**Phase (deg)**
u	0.0901	0
v	0.1493	0
w	0.8756	0
p	0.0101	0
q	0.0004	0
r	0.0032	0
ϕ	0.0036	0
θ	0.0001	0
φ	0.0011	0
Ω	0.4502	0

Table 3c Unstable low modulus oscillatory mode character

Eigenvalue 0.1009+0.4469i		
State	**Modulus**	**Phase (deg)**
u	0.7858	0
v	0.0920	162.2
w	0.2232	289.7
p	0.0096	3.0
q	0.0176	303.1
r	0.0050	301.2
ϕ	0.0213	284.7
θ	0.0386	225.8
φ	0.0101	224.6
Ω	0.5672	251.5

Finally, necessary conditions for the controllability of each mode can be established and used as a guide to the nature of gyroplane control. The "controllability matrix" is given by

$$C_r = E^{-1}B$$

It is obtained by applying the change of variable $x = Ez$ to the state-space description

$$\dot{\underline{x}} = A\underline{x} + B\underline{u}$$

e.g. see Ref. 7. The result is a state-space description

$$\dot{\underline{z}} = \Lambda\underline{z} + C_r\underline{u}$$

where Λ is a diagonal matrix whose elements are the eigenvalues of A. Hence a zero row of the matrix C_r indicates that the corresponding mode is uncontrollable. Alternatively, the relative magnitude of the elements in each row gives some indication (per unit control deflection) of which controls have the most influence over that eigenvalue, and hence mode. Table 4 shows that the large

modulus aperiodic mode controllability is dominated by longitudinal cyclic, while the dutch roll-type mode controllability is dominated by lateral cyclic and rudder, and somewhat surprisingly, longitudinal cyclic. The unstable low modulus mode is most strongly influenced by longitudinal cyclic although the inherent cross-coupling is such that the lateral cyclic has almost as large an effect.

Table 4 controllability of selected modes

	δ_r	θ_{1s}	θ_{1c}	δ_t
	Magnitude			
Eigenvalue -0.4243+3.9088i	10.0226	25.4127	7.2301	4.7145
Eigenvalue -2.8248	1.1708	277.2258	21.8408	11.9258
Eigenvalue 0.1009+0.4469i	2.6785	184.6675	135.8853	14.3250

Response to control inputs

The short-period response to longitudinal cyclic, or pitch, inputs is examined in this section. This response was chosen for two reasons: first, because of its importance to handling qualities; second, because the stability analysis revealed this mode to be unconventional in the helicopter or aeroplane context.

The full non-linear model with simulation of individual blades was used. Figure 9 shows the form of the longitudinal cyclic input as a doublet of 2s period. Three amplitudes were used: 0.45, 0.9 and 1.8 deg. Figure 10 shows the pitch rate response to each input. For comparative purposes, the responses are normalised by dividing pitch rate by the corresponding amplitude of input. This clearly renders any amplitude-dependent non-linearities. These inputs produce a wide range in the magnitude of pitch rate response. The smallest amplitude for example, produces a peak pitch rate of around 3 deg/s, while the largest input produces about 12 deg/s. It can be seen that there is some non-linearity with input size, but it is not very significant for the range of input magnitudes examined. The result also highlights another aspect of the short-period pitch response, and that is the apparent lack of pitch damping - the response increases almost uniformly with time after each step of the doublet input.

Analysis

The most significant item highlighted in the results is the short-period pitch motion of the gyroplane. The stability analysis and the time responses show that a classical short-period mode does not exist, either in terms of mode damping and frequency, modal content or angular response. An examination of the stability matrix A (i.e. the stability derivatives) and the gyroplane configuration, is necessary to understand this behaviour.

The 80 knot case is again used as an example. The classical approximation to the short-period mode for aeroplanes and single main and tail rotor helicopters with small offset flapping hinges (Ref. 8) is given by the minor of A

$$A_{sp} = \begin{bmatrix} Z_w & Z_q \\ M_w & M_q \end{bmatrix}$$

The appropriate values of the derivatives are

$$Z_w = -2.912$$
$$M_w = -0.013$$
$$Z_q = 46.178$$
$$M_q = 0.118$$

Note that the pitch damping M_q is very small, and positive, and will therefore tend to be destabilising. This explains the pitch rate response shown in Figure 10. The derivative M_w is negative i.e. stabilising. This is opposite to that normally obtained with helicopters without tailplanes, Ref. 9. The derivative Z_q is dominated by the speed (80 knots or 41.184 m/s) so about 10% of its value comes from rotor aerodynamics, usually taken to contribute negligibly to this derivative, Ref. 9. The derivative Z_w is of the correct magnitude for a rotor at this speed and thrust.

These values give approximate eigenvalues of A_{sp} of -0.0950 and -2.6990, the latter very close to the exact value of -2.8248. The exact value for the former eigenvalue is about -0.3, but it tends to coalesce with the rotorspeed mode to produce a complex conjugate pair, seen in Figure 8 as

the squares. Although this approximation to the short-period mode is only partially valid, it can be used to explain how the two real roots tend to be produced. If the mode were conventional, it would be oscillatory in nature. The condition for a pair of real roots being produced is

$$(Z_w M_q - M_w Z_q) < (Z_w + M_q)^2 / 4$$

This is satisfied here since not only is the product $Z_w M_q$ small in magnitude, it is less than zero, making an added contribution toward satisfying the condition for two real roots.

The key feature that explains this unconventional short-period mode is then the pitch rate damping M_q . Its positive value can be attributed to a substantial aerodynamic contribution to Z_q arising from the rotor not being at the pitch rotation centre (the c.g.). Since the c.g. is forward of the hub, the moment contribution from this source is positive, i.e. destabilising. This is opposite to the conventional helicopter with its forward shaft tilt. The c.g is forward of the hub since it has been chosen to lie on the shaft line to give a reasonable pitch attitude in cruise, and the shaft itself is tilted aft by 5 deg.

Similar reasoning explains the negative value of M_w. It is dominated by the moment contributed from Z_w , i.e. negative with the c.g. forward of the rotor hub.

Discussion

One interesting aspect of this study has been the usefulness of the model in the form of classical rigid-body linearised stability and control derivatives. The development of rotorcraft mathematical modelling has been such that improved fidelity has only been possible by including non-linearity and additional degrees of freedom, thereby rendering derivative models apparently inappropriate. This study helps to show however, that a derivative model that has been numerically reduced from an individual blade/blade element formulation, captures the rigid-body response characteristics of the full model. The value of the derivative is that it provides a mechanism by which understanding and analysis of physical behaviour can be made, which is essential for sophisticated

models such as the one used for this study. The stability and control derivative therefore still has a role to play in the analysis of rotorcraft flight dynamics.

The derivative form of the model has been essential for developing an understanding of the gyroplane's behaviour. It has characterised complex behaviour in a manner that allows explanation of response characteristics, particularly the short-period longitudinal motion. The nature of key terms in the pitching moment equation i.e. M_q and M_w was shown to be opposite to that experienced with the helicopter, and this is due to the fact that the rotor shaft is tilted aft, rather than forward. This could be considered to be a design driver, since the rotor disc needs to be at a positive angle of attack for autorotative flight and tilting the shaft aft reduces the amount by which aircraft nose-up pitch attitude is needed to provide this. It is an example of how vehicle configuration affects gyroplane flight mechanics.

Increased flapping hinge offset would tend to stabilise M_q. However the gyroplane in this study had a deliberately low offset to mimic the rotor systems of contemporary gyroplanes. The analysis of gyroplane flight mechanics in pitch conducted in this Paper may be valid, since Ref. 2 quotes a survey of owners who highlight sensitivity in pitch to be a noticeable handling feature. Changing the rotor system to allow increased flap hinge offset could result in a more complex (and hence costly) design than is currently used. Bearingless main rotor technology such as that currently under development for helicopters however may allow low cost higher-offset rotors to become available for the homebuilt gyroplane in the future. This could benefit airworthiness and flight safety through improved handling qualities, but full validation of this model from flight test including handling assessments would be required before such a design change could be justified on these grounds.

It is also clear that the rotorspeed degree of freedom must be included in modelling gyroplane flight. This is not always the case with helicopters where the engine and rotor governing system can often be assumed to produce a constant rotorspeed, irrespective of flight condition. Analysis of the

character of the modes shows that the rotorspeed state is not restricted to the rotorspeed mode, but appears as a substantial response in the short-period and longer-term unstable longitudinal modes as well. The rudimentary analysis of the rotorspeed mode conducted at the start of this Paper provides a surprisingly good approximation to the actual value of this mode's eigenvalue, which is about -0.25. The expression for k_Ω could therefore be used in parametric exercises to establish the impact of design variables on the stability of this important mode.

Conclusions

Gyroplane flight mechanics are such that the trim characteristics and rigid-body dynamics are similar to those of a conventional single main and tail rotor helicopter. There are lightly-damped modes with cross-coupled responses, and the response to controls displays non-linearity with input magnitude. Conventional helicopter mode types are present e.g. modes with discernible dutch roll or phugoid characteristics. However, rotorspeed is an important additional degree of freedom that must be included in modelling gyroplane flight mechanics. This is because the coupling between rotorspeed and the rigid-body states is such that the rigid-body modes have a considerable rotorspeed content. Only in one aspect of longitudinal trim i.e. the pitch attitude variation with airspeed, is the gyroplane similar to a fixed-wing aeroplane. The short-period pitch motion, important from a handling qualities standpoint and which was studied in detail, is unlike either the aeroplane or helicopter. This was attributed to negligible pitch rate damping M_q . For the configuration studied, with moderate aft tilt of the shaft, this result is attributed to rotor force perturbations with pitch rate being destabilising. Rotor force perturbations with vertical velocity (or angle of attack) tend to be stabilising. This is opposite to the helicopter case.

References

1) Prouty, R. W., *Helicopter Performance, Stability and Control*, 2nd. ed., Krieger, Malabar, 1990, pp. 142-146.

2) Anon, "Airworthiness Review of Air Command Gyroplanes", Air Accidents Investigation Branch Report, Sept. 1991.

3) Houston, S., "Rotorcraft Aeromechanics Simulation for Control Analysis - Mathematical Model Definition", University of Glasgow Dept. of Aerospace Engineering Report No. 9123, 1991.

4) Kim, F.D., et al, "Forward Flight Trim Calculations and Frequency Response Validation of a high Order Helicopter Simulation Model", *Proceedings of the 47th. Annual Forum of the American Helicopter Society*, Phoenix, May 1991, pp. 155-168.

5) McVicar, J.S.G., "A Generic Tilt-Rotor Simulation Model with Parallel Implementation", University of Glasgow Ph.D. Dissertation, Feb. 1993.

6) Achar, N. S., Gaonkar, G. H., "Helicopter Trim Analysis by Shooting and finite Element Methods with Optimally Damped Newton Iterations", *AIAA Journal*, Vol. 31, No. 2, Feb. 1993, pp. 225-234.

7) Richards, R. J., *An Introduction to Dynamics & Control*, Longman, London, 1979, pp.312-313.

8) Padfield, G. D., "On the Use of Approximate Models in Helicopter Flight Mechanics", *Vertica*, Vol. 5, No. 3, 1981

9) Bramwell, A. R. S., *Helicopter Dynamics,* Arnold, London, 1976, pp. 196-209.

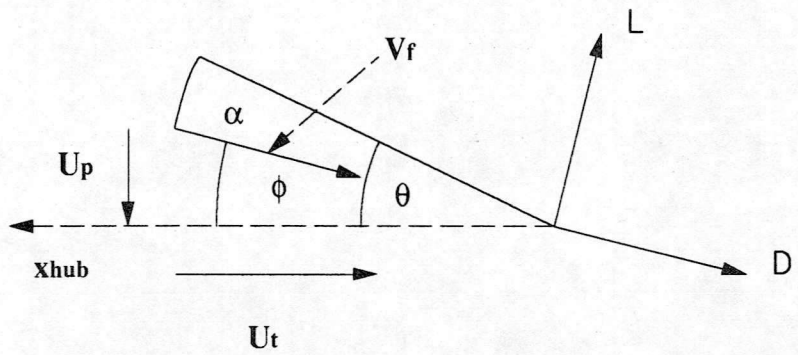

Figure 1 Schematic of blade element forces and velocities in helicopter mode

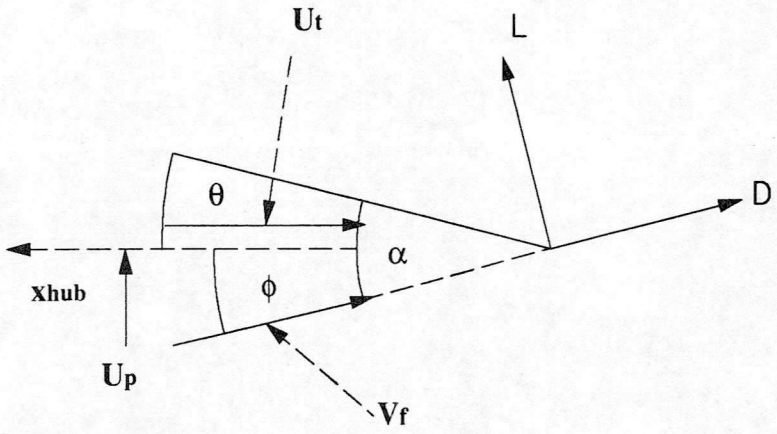

Figure 2 Schematic of blade element forces and velocities in gyroplane mode

Figure 3 Vertical acceleration in trimmed flight at 80 knots

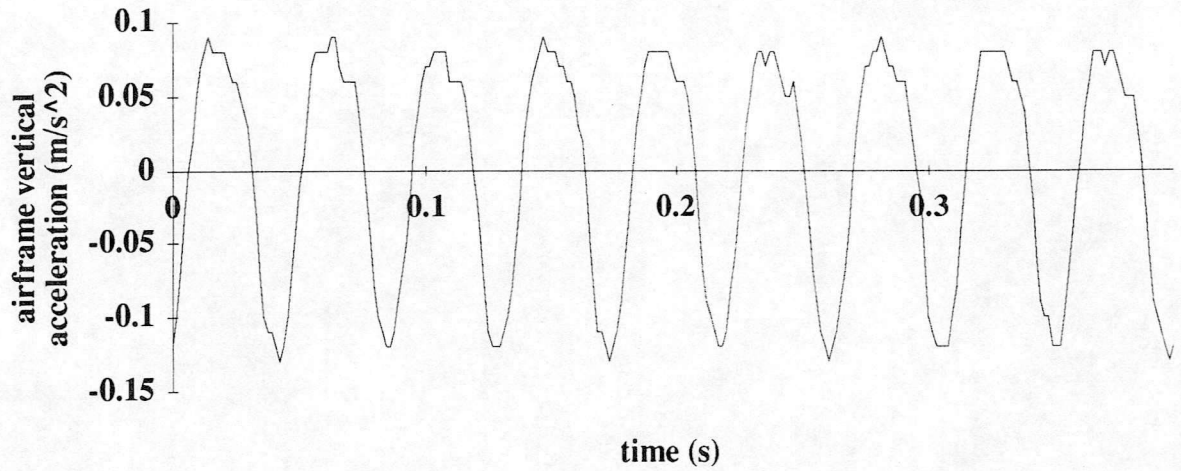

Figure 3

Figure 4 Rotorspeed response following release from pseudo-trim, 80 knots

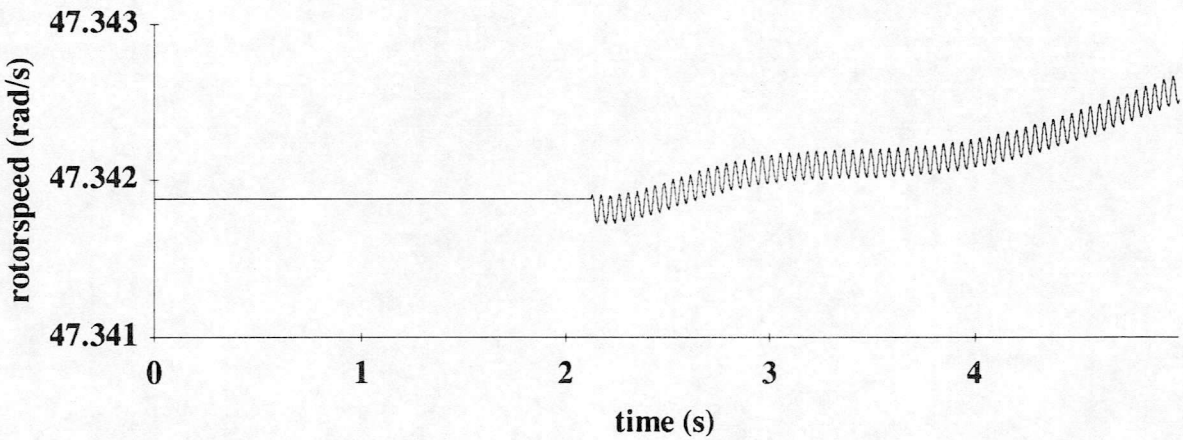

Figure 5 Aircraft control angles required to trim in level flight

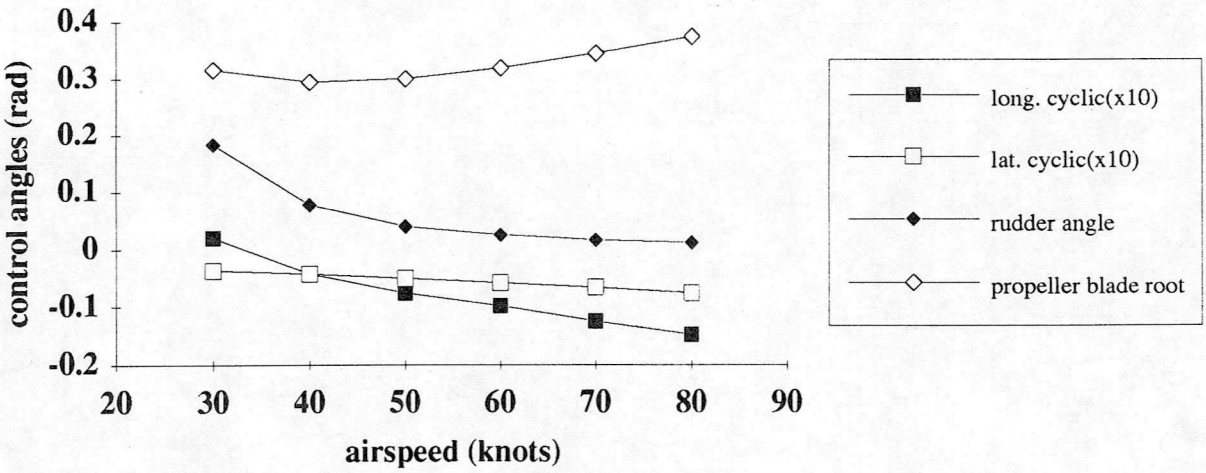

Figure 5

Figure 6 Aircraft attitudes required to trim in level flight

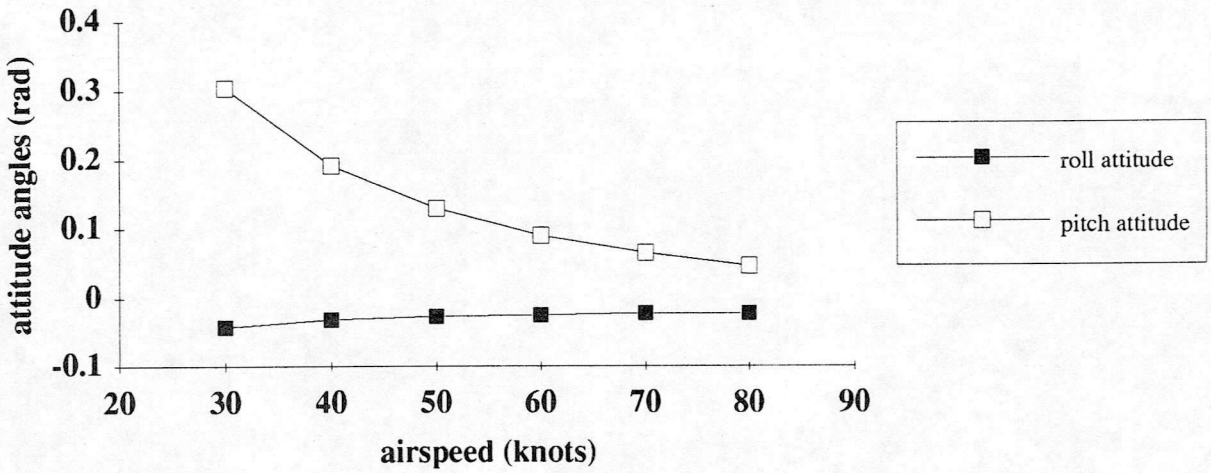

Figure 6

Figure 7 Rotorspeed resulting from trim in level flight

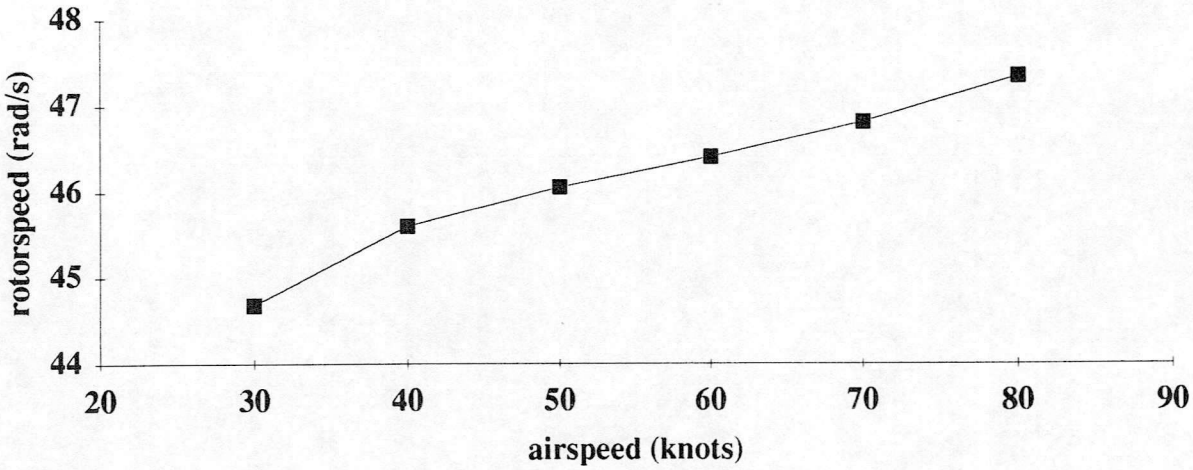

Figure 8 Locus of rigid-body mode stability roots, 30-80 knots

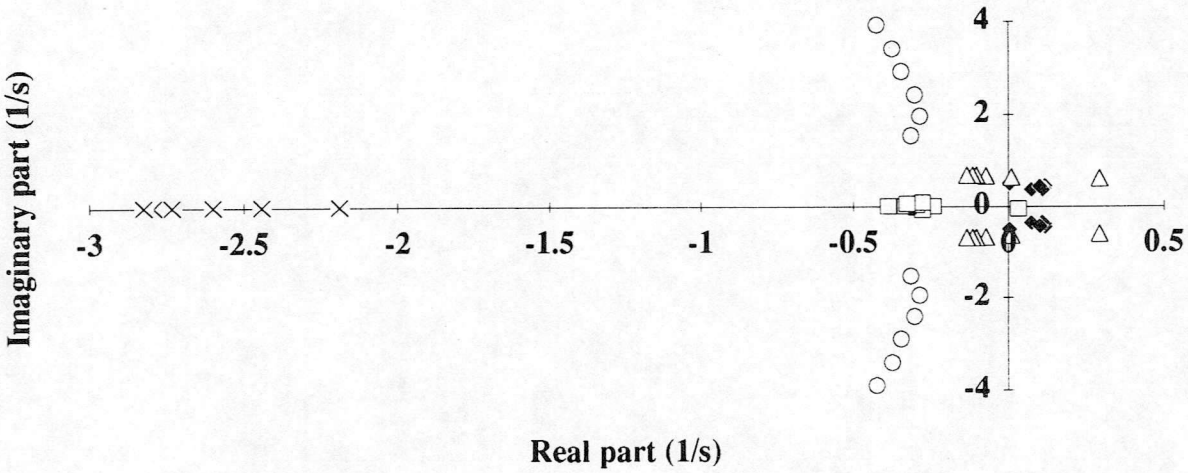

Figure 8

Figure 9 Longitudinal cyclic pitch control input

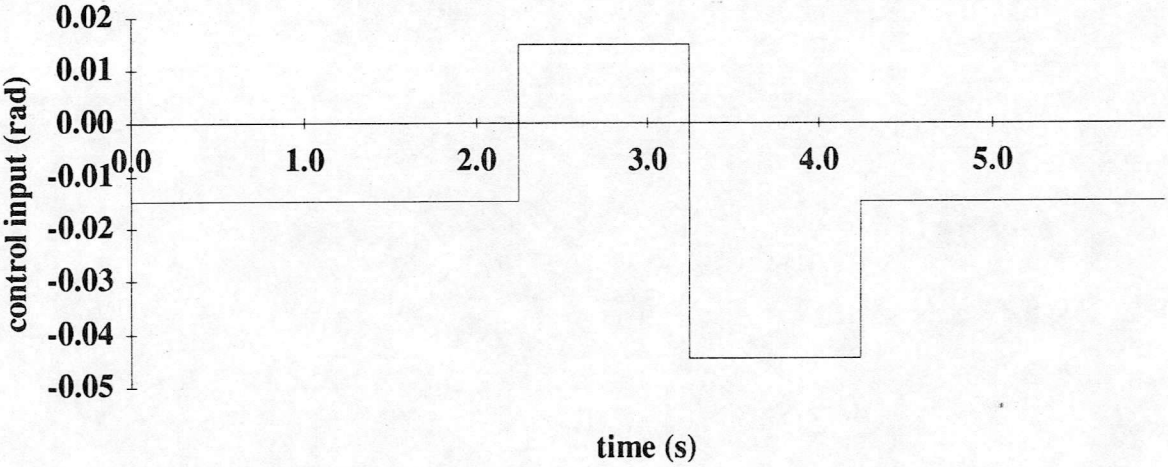

Figure 10 Normalised pitch rate response to different amplitude inputs at 80 knots

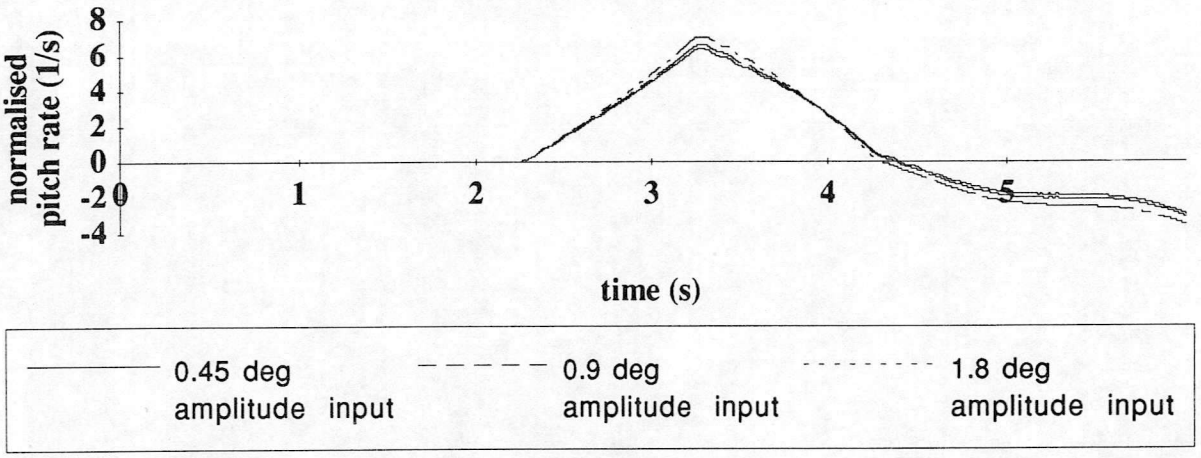

Figure 10